Copyright © 2014, American-Eurasian Network for Scientific Information publisher

American-Eurasian Journal of Sustainable Agriculture
ISSN: 1995-0748

JOURNAL home page: http://www.aensiweb.com/aejsa.html 2014 Special; 8(7): pages 62-68.

Published Online 2014 February 30. **Research Article**

Diesel Performances During Combustion using high Swirling Flow in Unconfined Burner

[1,2]Norwazan, A.R. and [2]Mohd Jaafar, M.N.

[1]*Faculty of Engineering, Universiti Pertahanan Nasional Malaysia, Kem Sg. Besi, 57000, Kuala Lumpur.*
[2]*Faculty of Mechanical Engineering, Universiti Teknologi Malaysia, 81310, UTM Skudai, Johor Bahru.*

Received: 25 June 2014; **Received**: 8July 2014; **Accepted**: 10 August May 2014; **Available online:** 30 August 2014

© 2014 AENSI PUBLISHER All rights reserved

ABSTRACT

This paper presents a numerical simulation of temperature profiles and CO formation along the combustor in the unconfined burner. Combustion flows with three different swirl angles using axial swirler are used to demonstrate the effect of temperature profiles on the center recirculation zone. The significance of the center recirculation zone is to ensure a good mixing of air and fuel in order to get a better combustion. A numerical study of non-premixed flow in the burner region is performed using ANSYS Fluent. The Reynolds–Averaged Navier–Stokes (RANS) realizable k-ε turbulence approach method was applied with the eddy dissipation model. The paper focuses the flow field behind the axial swirler downstream that determined by transverse flow field at different on radial distances. The inlet velocity, U_0 is 30 m/s entering into the burner through the axial swirler that represents a high Reynolds number. The results of temperature and CO formation were plotted against radial distance. Both profiles are different after undergoing the different swirler up to the burner exit. However, the results of each profile showed that the high swirl angles gives better swirling flow patterns for both profiles

Keywords: burner, swirling flow, combustion, CO emissions, realizable *k-ε*

INTRODUCTION

Combustion is one of the most significant an exothermic reactions in engineering process involving heat transfer, turbulent fluid flow, and chemical reactions. Burner is widely used in most combustion industrial while the swirler is associated to merge and ensure the two streams of air and fuel have a good mixing. Besides that, the demand of combustion efficiency in burner increased. The burner also needs to be minimized the pollutant emission products. Swirlers are used as flame holders to control the mixture speed depending on the flame speed [1]. In addition, generating a swirling flow inside burners enhances the mixing of the different constituents of the mixture permitting, thus, a better control of the combustion process in terms of flame quality and pollutants emission. The priority concern in development of combustor is very low pollutant emission product of CO and NO_x. During combustion, CO is produced in substantial amounts and subsequent oxidation to CO_2 is retarded until HC radicals and fragments have been consumed [2]. Han *et al*., [3] mentioned that combustion temperature influences CO emissions, but the temperature decreases below 1500 K, then the CO rapidly decreases.

Turbulent swirling flow in the burner plays an important role in controlling the combustion processes and performances and it will reduce the emission products. Swirling flows have been investigated extensively that used in all kinds of practical combustion systems including gas turbine combustor of aero-engine and industrial, swirl burner, furnaces, cyclone combustor and others [4,5]. Consequently, the flame structure and stability in combustion is extremely dependent on the aerodynamics and mixing characteristics of fuel and oxidizer in their mixing region [5,6,7,8]. A swirling flow is the cause of an impartation of a tangential

Corresponding Author: Norwazan, A.R., Faculty of Engineering, Universiti Pertahanan Nasional Malaysia, Kem Sg. Besi, 57000, Kuala Lumpur ,
Tel: 603-90513400; E-mail: norwazan@upnm.edu.my

component by usage of swirler positioned within the burner [7,9]. The appropriate of swirl produces a large adverse pressure gradient in the direction of flow, which promotes the reverse flows. Thus, the formation of a flow pattern provides an aerodynamic blockage and reduced velocities necessary to stabilize the flame [6,7].

The prediction of the swirling flow characteristics in the combustor can be done using numerical simulation in order to optimize the design. A numerical study on the application of computational fluid dynamics (CFD) is a great potential in order to investigate isothermal and combustion process. Turbulence models that are great practical importance are three-dimensional and time-dependent. Computational methods of solving the differential equations of fluid dynamics are well advanced [10]. Turbulent behavior of inertial systems at every time in the space continuum seems to appear similar characteristics such as vortex structures and structural inhomogeneties [11]. Turbulent is the state of fluid processing a non-regular or irregular motion such that velocity at any point may vary both in magnitude and direction with time. Turbulent motion is accompanied by the formulation of eddies and the rapid interchange of momentum in the fluid.

The swirl intensity is generally characterized by the swirl number, defined as the ratio of the axial flux of azimuthal momentum to the axial flux of axial momentum [18,12,13,14,15,16,]. The swirl number is a measure of the strength of the swirling flow [17] as a main parameters used to characterize swirling flow [18]. Generally, the swirl number above 0.6 is indicated as a strongly swirling flow [19]. The swirl number is defined as:

$$S = \frac{G_\theta}{G_x R} \tag{3}$$

where,

$$G_\theta = \int_0^R \rho(Wr)\, u 2\pi r\, dr \tag{4}$$

and

$$G_x = \int_0^R \rho U^2 2\pi r\ \ dr \tag{5}$$

where U,W and ρ are the axial velocity, tangential velocity and density respectively. For axial swirler, the swirl number is related to the swirl angle, θ, inner r_i and outer radius r_0 as given by [19] which the swirl number was proportional to tan ϕ [20]:

$$S_N = \frac{2}{3}\left[\frac{1-\left(\frac{r_i}{r_0}\right)^3}{1-\left(\frac{r_i}{r_0}\right)^2}\right]\tan\theta \tag{6}$$

Steady-state, incompressible, turbulent flows are governed by the Reynolds-averaged continuity and Navier-Stokes equations. The conservation form of these equations can be written as

Continuity:

$$\frac{\partial U}{\partial z} + \frac{1}{r}\frac{\partial}{\partial r}(rV) = 0 \tag{7}$$

Axial Momentum:

$$U\frac{\partial U}{\partial z} + V\frac{\partial U}{\partial r} = -\frac{1}{\rho}\frac{\partial p}{\partial z} + v\left(\frac{\partial^2 U}{\partial z^2} + \frac{1}{r}\left(r\frac{\partial U}{\partial r}\right)\right) - \frac{\partial}{\partial z}\langle u^2\rangle - \frac{\partial}{\partial r}\langle uv\rangle - \frac{\langle uv\rangle}{r} \tag{8}$$

In k-ε model the turbulent viscosity is computed by the combination of the turbulence kinetic energy, k and its dissipation rate, ε as follows

$$\mu_t = \rho C\mu \frac{k^2}{\varepsilon} \tag{9}$$

The two differential equations are used to describe the turbulence kinetic energy, k and dissipation rate of turbulence, ε in the realizable k-ε model, Eqs. (10) and (11), respectively [21]

$$\frac{\partial}{\partial t}(\rho k) + \frac{\partial}{\partial x_j}(\rho k u_j) = \frac{\partial}{\partial x_j}\left[\left(\mu + \frac{\mu_t}{\sigma_k}\right)\frac{\partial k}{\partial x_j}\right] + G_k - \rho\varepsilon - Y_m \tag{10}$$

and

$$\frac{\partial}{\partial t}(\rho\varepsilon) + \frac{\partial}{\partial x_j}(\rho\varepsilon u_j) = \frac{\partial}{\partial x_j}\left[\left(\mu + \frac{\mu_t}{\sigma_\delta}\right)\frac{\partial \varepsilon}{\partial x_j}\right] + \rho C_2 \frac{\varepsilon^2}{k+\sqrt{v\varepsilon}} \tag{11}$$

G_k represents the production of turbulence kinetic energy. The σ_k, σ_ε, $C_{1\varepsilon}$, $C_{2\varepsilon}$ and C_μ are model constants. Shih *et al.* claimed that the realizable k-ε model yields better results for rotating shear flows compared to standard k-ε model. This paper investigates the effect of axial swirler on the combustion performances and pollutant emissions. The axial swirler is adopted inside a burner and varied with different swirl vane angles. The studies are presented using transverse flow field in different radial distance after flow entering air swirler downstream towards end of outlet burner.

Materials and Methods

The CFD numerical simulations were performed with the ANSYS Fluent to solve the governing equations. In CFD, the fluid flow can be predicted through arbitrary geometries that gives solution of flow speed, pressures, flow pattern etc. Initially, the Computer Aided Design (CAD) modeling was created using *AutoCAD 2012* software in three-dimensional (3D) according to the actual laboratory scale of liquid fuel burner. In the present study, the numerical simulation of swirling flow, issuing from the inlet of a burner, using standard k-ε turbulence models is considered. The 3D CAD modeling was assembled and exported to produce meshing and set-up the boundary conditions. The meshing was composed primarily of tetrahedral mesh elements including hexahedral, pyramidal and wedge with various sizes. 3D Reynolds-Averaged Navier Stokes (RANS) computations modeling of the entire section including swirl generation system and burner have been performed using commercial CFD-software namely ANSYS *Fluent*. Fluent computer code uses a finite-volume procedure to solve the RANS

equations of fluid flow in primitive variables such as axial velocity, radial velocity and tangential velocity.

This study was focused on the eddy dissipation concept model whereas is widely used for turbulence modeling and adopted for non-premixed combustion modeling. This combustion chemistry modeling using eddy dissipation model is operated as mixed-is-burned concept, relies on the accurate turbulence prediction more than any other chemistry model. A 3D computational grid of 1.5 million cells was employed for the realizable *k-ε* model simulation in order to simulate the combustion flow in unconfined burner. The model constants for the realizable *k–ε* model are C_{μ} = 0.09, $C_{1\varepsilon}$ =1.44, $C_{2\varepsilon}$ =1.92, and wall Prandtl number =1. The First Order Upwind Scheme was set for spatial resolution. The all RANS model were discretized using Quadratic Upstream Interpolation for Convection Kinetics (QUICK) and the SIMPLE algorithm was used.

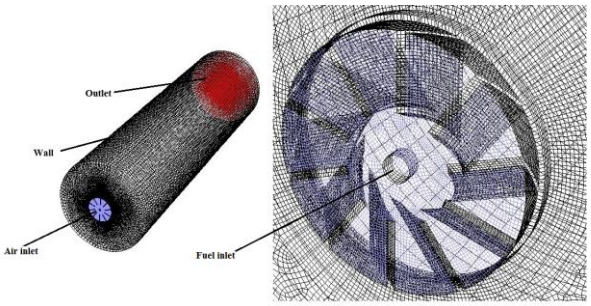

Fig. 1: The mesh modeling of unconfined burner including the axial swirler.

At the front of burner, the air and fuel inlet and swirler are located with the element mesh were built in fine grids as shown in Figure 1. The burner with axial swirler has an outer diameter of 280 mm and the swirler diameter is 73 mm. The length of burner is 1000 mm. In this analysis, the fuel/air ratio evaluated is 1.0 The boundary condition of both air and fuel inlet assigned as mass flow rate are 0.01109 and 0.000954 kg/s for three different swirler number. The transverse flow field data were measured at different location of burner length at *z*-planes. In this study, 3 different swirl numbers are studied including S_N = 0.436, S_N = 0.630 and S_N = 0.895 represented as a swirl vane angles of 30, 40 and 50 degree.

Results and Discussion

Figure 2 shows the temperature distribution along the inside of the burner in difference of swirl vane angles. The experimental data is plotted for axial swirler of 40 degree angle. The maximum temperature patterns are slightly same but the peak of maximum temperature of experimental data is deferred after 200 mm downstream. For the numerical results are shown that the peaks of maximum temperature are occurred approximately after 100 to 200 mm from the inlet point. From the graph, the diesel combustion in the unconfined burner with the axial swirler of 50 degree angle showed the highest temperature and it is happened early compared the other angles.

Figure 3 shows the comparison of transversal temperature profiles in radial distance. In early stage of combustion, at x/D = 0.1 the highest temperature was obtained by using high swirl vane angles. The temperature profiles keep increased in axial direction and to the wall but the temperature was highly increased in the center core of a combustion burner. At x/D = 0.5, it shows that the peak of temperature for swirl angle of 40 and 50 degree has a highest temperature value and keeps reduced in x/D = 0.6. In x/D = 0.5 the flames temperature are shown more stabilize but the temperature of swirl angle of 30 degree still increased. The flame temperature of high swirl angle is highest and bigger than the low swirl angle temperature was occurred earlier in axial position. The low temperature for low swirl angle was decreased at x/D = 0.6 to the downstream but slightly slow compared with the high swirl angle. In overall the tread for each swirl angle are similar.

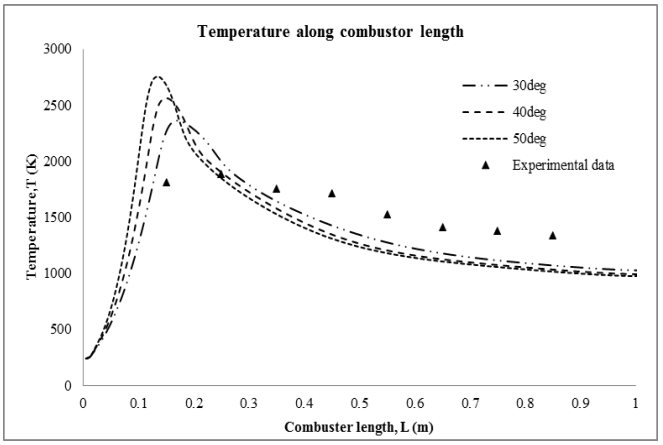

Fig. 2: Comparison temperatures along combustor length between experimental and numerical data.

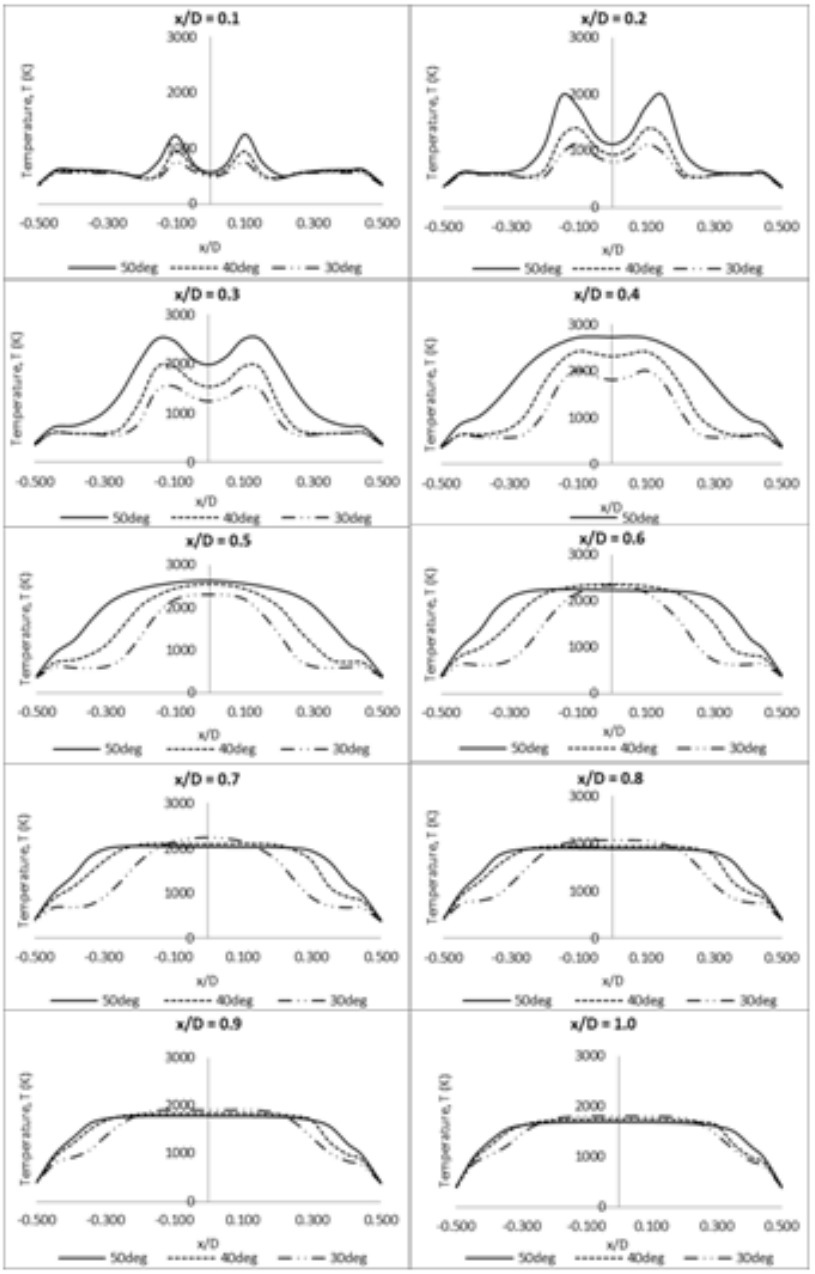

Fig. 3: Transversal profiles of temperature at different radial distance.

The total carbon monoxide (CO) profiles in Figure 4 showed that the differences of each swirl angle as temperature profiles. This CO formation inside burner occurred due to combustion, which is a high swirl angle gives highest CO formation at x/D = 0.4. High concentration of temperature at x/D = 0.5 cause the CO re-burned to convert CO_2 and CO slowly reduced when temperature reduced, obviously for 50 degree swirl angle profile. The CO formation of high swirl angle is quite wide spread near to the wall. It might be caused by the high turbulent flow entering into the chamber and slow combustion occurred. While the low swirl angle produced low CO formation and keep increased till x/D = 0.8. Thus, CO was reduced after x/D = 0.9 and become wide spread near to the wall. The trends of each CO formation are similar. Both Figure 3 and 4 illustrated the temperature and CO profiles are parallel for each swirl vane angle.

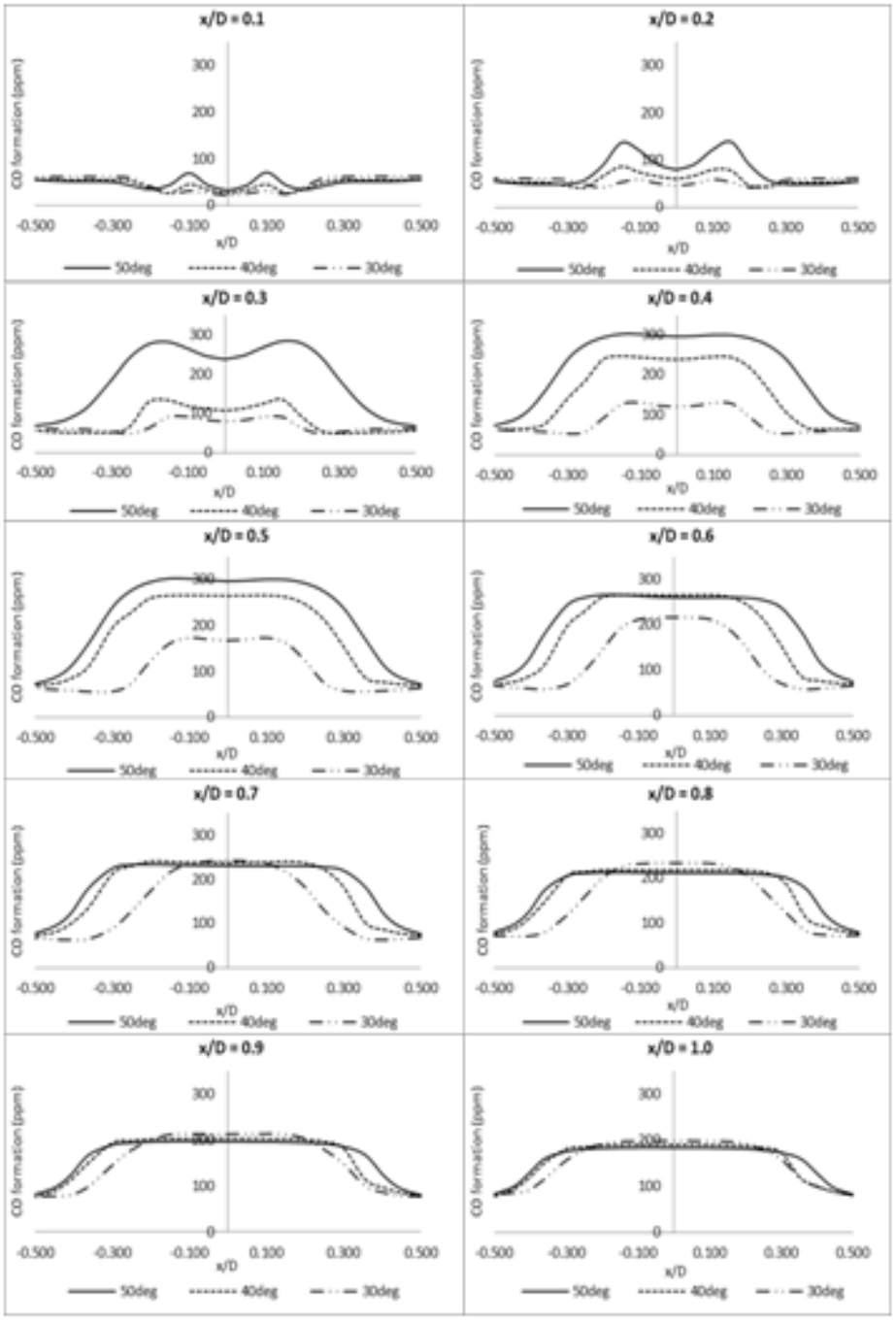

Fig. 4: Transversal profiles of CO formation at different radial distance.

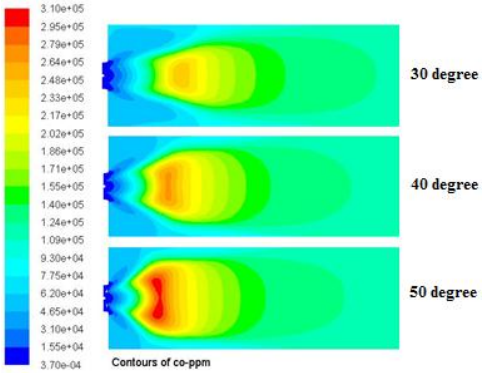

Fig. 5: CO contour of different swirl angles.

Figure 5 shows the contour of CO formation for each swirl angles. This contour presented that the low swirl angle has small contour and length is slightly longer compared with the high swirl angle has a wide and shorter length contour. The high swirl angle also shown the CO formation occurred near to the swirler throat compared in low swirl angles. For low swirl angles, the flame is far from the swirler throat compared the high swirl angles.

Conclusion:

The realizable *k-ε* turbulence approach method was used in this study to evaluate the axial swirler adopted inside an unconfined burner are well compared. The simulation is defined the temperature and CO formation profiles with the various swirl numbers. This study also was investigated to determine better CO emissions suitable with vane angle of axial swirler using realizable *k-ε* turbulence model due to combustion process. The graph temperature and CO formation are shows that the obvious different are occurred at the early *z*-planes after the flow entering the burner throughout the axial swirler. Concurrently, the temperature profiles is increased, the CO is also increased but it is depends on the swirl angles. It can be concluded that, the high swirl angles, the profiles are changed faster than the low swirl angles.

Acknowledgments

The authors would like to thankful to Ministry of Science, Technology and Innovation (MOSTI) for their funding under Sciencefund Grant 4S046 as well as UTM for their supports.

Authors' Contribution:

Dr Mohammad Nazri had developed an ideas, provided the material and facilities. Norwazan had performed the combustion analysis using CFD software, run the experiment and analyze the data.

References

1. Mohd Jaafar, M.N., K. Jusoff, M.S. Osman and M.S.A. Ishak, 2011. Combustor Aerodynamics Using Radial Swirler, *International Journal of Physics Sciences, 6(13): 3091-3098.*
2. Zanforlin, S., R.D. Reitz and R. Gentili, 1999. Studying the roles of kinetics and turbulence in the simulation of diesel combustion by means of an extended characteristics time model, *International Congress and Exposition Detroit, Michigan, 1-4.*
3. Han, D., A.M. Ickes, S.V. Bohac, Z. Huang and D.N. Assanis, 2012. HC and CO emissions of premixed low-temperature combustion fueled by blends of diesel and gasoline, *Fuel, 99: 13-19.*
4. Ridluan, A., S. Eiamsa-ard and P. Promvonge, 2007. Numerical simulation of 3D turbulent isothermal flow in a vortex combustor. *International Communication in Heat and Mass Transfer, 34: 860-869.*
5. Litvinov, I.V., S.I. Shtork, P.A. Kuibin, S.V. Alekseenko and K. Hanjalic, 2013. Experimental study and analytical reconstruction of processing vortex in a tangential swirler, *International Journal of Heat and Fluid Flow, 42: 251-264.*
6. Syred, N. and J.M. Beer, 1974. Combustion in Swirling Flows: A Review, *Combustion and Flame, 23: 143-201.*
7. Sloan, D.G., P.J. Smith and L.D. Smoot, 1986. Modeling of swirl in turbulent flow systems. *Prog. Energy Combustion Science, 12: 163-250.*
8. Eldrainy, Y.A., M.N. Mohd Jaafar and T. Mat Lazim, 2008. Numerical investigation of the flow inside primary zone of tubular combustor model, *Jurnal Mekanikal, 26: 162-176.*
9. Yegian, D.T. and R.K. Cheng, 1998. Development of a vane-swirler for use in a low NO_x weak-swirl burner. *Combust. Sci. Technol, 139(1–6): 207-227.*
10. Launder, B.E. and D.B. Spalding, 1974. The

numerical computation of turbulent flows. *Computer Methods in Applied Mechanics and Engineering, 3: 269-289.*

11. Magnussen B.F. and B.H. Hjertager, 1976. On mathematical modeling of turbulent combustion with special emphasis on soot formation and combustion, *16th Symposium (International) on Combustion, Combustion Institute, pp: 719-729.*
12. Eldrainy, Y.A., K.M. Saqr, H.S. Aly and M.N. Mohd Jaafar, 2009. CFD insight of the flow dynamics in a novel swirler for gas turbine combustors, *International Communications in Heat and Mass Transfer, 36: 936–941*.
13. Orbay, R.C., K.J. Nogenmyr, J. Klingmann and X.S. Bai, 2013. Swirling turbulent flows in a combustion chamber with and without heat release, *Fuel, 104: 133-146.*
14. Pollard, A., H.L.M. Ozem and E.W. Grandmaison, 2005. Turbulent, swirling flow over an asymmetric constant radius surface. *Experimental Thermal and Fluid Science, 29: 493-509.*
15. Beltagui, S.A., A.M.A. Kenbar and N.R.L. Maccallum, 1993. Comparison of Measured Isothermal and Combusting Confined Swirling Flows: Peripheral Fuel Injection, *Experimental Thermal and Fluid Science, 6: 147-156.*
16. Bourgouin, J.F., J. Moeck, D. Durox, T. Schuller and S. Candel, 2013. Sensitivity of swirling flows to small changes in the swirler geometry, *C. R. Mecanique, 341: 211–219.*
17. Murphy, S., R. Delfos, M.J.B.M. Pourquie, Z. Olujic, P.J. Jansens and F.T.M. Nieuwstadt, 2007. Prediction of strongly swirling flow within an axial hydrocyclone using two commercial CFD codes, *Chemical Engineering Science, 62: 1619-1635.*
18. Syred, N., M. Abdulsada, A. Griffiths, T.O. Doherty and Bowen, 2012. The effect of hydrogen containing fuel blends upon flashback in swirl burners, *Applied Energy, 89: 106-110.*
19. Grech, N., C. Koupper, P.K. Zachos, V. Pachidis and R. Singh, 2012. Consideration on the numerical modeling and performance of axial swirlers under relight conditions, *Journal of Engineering for Gas Turbines and Power.*
20. Beer, J.M. and N.A. Chigier, 1972. Combustion Aerodynamics. *Applied Science Publishers Ltd*.
21. Rohani, B. and K.M. Saqr, 2012. Effects of hydrogen addition on the structure and pollutant emissions of a turbulent unconfirned swirling flame, *International Communication in Heat and Mass Transfer, 39: 681-688*.